Localizing and Identifying Underground Objects using Gravitational Measurements †

Carlos H. Muravchik

LEICI, Fac. de Ingeniería
Univ. Nac. de La Plata
1900 La Plata, Argentina

Arye Nehorai

Department of Electrical Engineering
Yale University
New Haven, CT 06520

Abstract

We consider the problem of localizing underground objects and identifying their parameters by measuring the components of the gravity gradient tensor. Applications are oriented towards finding tunnels, pollutants and aquifers, archaeology, oil exploration, verifying compliance with peace treaties (e.g. missile inspection), etc.

Close interaction between the physical model and a signal processing approach leads to a source location and parameter estimation problem. We propose several modeling alternatives to solve the non-uniqueness of the inverse problem, though this paper includes only point masses.

We use a maximum likelihood procedure to solve the parameter estimation problem. The Cramér-Rao bound is computed and presented for the range and mass of a spheroidal object. Estimation bounds on the location of a single point mass and the resolution for two point masses are studied.

1 Introduction

We consider the problem of localizing underground objects and identifying their parameters using measurements of the components of the gravity gradient tensor. Consider for instance the case of having to find a tunnel, an oblong object less dense than its surroundings. Assuming we have detected it, *i.e.* we have an idea of where it might be, we need to estimate its precise location. The direction along which the tunnel runs, *i.e.* its orientation, is often needed. We may also require to estimate its mass density, since it might be confused with other oblong objects of different density, such as aquifers.

We foresee applications of our approach to archaeology, oil exploration, mineralogy, determination of the geode, localization of pollutants and aquifers, etc. Other interesting applications of gradient gravimetry are given in [5], *e.g.* inspection of missiles.

Assume a certain mass distribution is given, producing a gravitational potential and force field. A test mass at a certain location $\vec{p}$ experiences an attractive force due to this field, $\vec{F}(\vec{p})$. The gravitational field is the attractive force per unit mass and the gravitational gradient is given by the partial derivatives of each gravitational field component, then

$$G(\vec{s}) = \begin{bmatrix} G_{xx} & G_{xy} & G_{xz} \\ G_{yx} & G_{yy} & G_{yz} \\ G_{zx} & G_{zy} & G_{zz} \end{bmatrix}_{|\vec{s}}$$

is usually called the gradient tensor at location $\vec{s}$. A convenient unit of measurement for the gravitational gradient is the *Eötvös* and is equivalent to $1E = 10^{-9} sec^{-2}$. If the Earth were a uniformly dense sphere, the gradient at any point of its surface would be vertical with an intensity of about 3100 E.

Several sensors for measuring the gravity gradient (gradiometers) have been described and studied in the literature. We shall consider using an instrument based on a spinning wheel with accelerometers, described in detail in [3]. The output of the instrument has two signals: the *in-line gradient* and *cross gradient*. When the rotating wheel is laid horizontally the in-line gradient is given by $G_{yy} - G_{xx}$ and the cross gradient by G_{xy}. It is also possible to slant the rotating wheel in other orientations and we can show (see [4]) that there exists a matrix $\mathbf{M_j}$ such that

$$g_j(k) = \mathbf{M_j} \, [G_{xx} \; G_{xy} \; G_{xz} \; G_{yy} \; G_{yz} \; G_{zz}]^T_{|\vec{s}_k}$$

†This work was supported by the Air Force Office of Scientific Research under Grant no. F49620-93-1-0096, the Office of Naval Research under Grant no. N00014-91-J-1298, the National Science Foundation under Grant no. MIP-9122753 and by Schlumberger-Doll Research. CHM is a member of Comis. de Investig. Cientif. de la Pcia. de Buenos Aires (CICPBA).

where $g_j(k)$ is a vector with two components, the inline and cross gradient at the location $\vec{s}_k$, and with the rotating wheel in the j-th orientation. The formula reflects the fact that the gradient tensor is symmetric. Moreover, Poisson's equation introduces a further constraint among the diagonal components of the gradient tensor, leaving only five independent components.

Assume we have detected, in a certain region, the presence of the mass distribution pattern for which we are looking and we have to estimate its parameters. We take a number of gravitational gradient measurements at certain locations on the Earth's surface, with the gradiometer slanted in different orientations. Our modeling approach, explained in §2, allows us to formulate the parameter estimation problem in an array processing setting, making available many results from that context. We use a maximum likelihood estimation scheme to obtain estimates of location, orientation and mass. We also compute the Cramér-Rao lower bound and use it to gain some insight into the capabilities of our method.

2 Modeling

Assume a cartesian coordinate system is adopted at the reference measurement point (MP_1), as indicated in fig. 1. The z axis is roughly along the vertical and the xy-plane is parallel to the surface. Other measurement points MP_k are placed at locations $\vec{s}_k$ for $k = 2, \ldots, K$. We show in [4] that a precision on the parallelism of the frames of about a minute of angle per axis gives acceptable results and this can be achieved with standard geodesic equipment.

Underground masses (white circles) are located with their centers of mass $\{\mathrm{CM}_1, \mathrm{CM}_2, \ldots\}$ at positions $\{\vec{p}_1, \vec{p}_2, \ldots\}$. The overall potential function is the sum of the contributions of these masses, plus the effect of a homogeneous ground of uniform density and its spurious objects (black circles), such as stones, holes, rocks, etc. The object of interest, as well as the undesired masses, can be detected from the surrounding ground as long as their densities differ from the background density.

Write the total gradient tensor due to the background, distributed masses indexed by l and discrete point masses indexed by i, as follows:

$$G(\vec{s}) = \sum_l \int_{\vec{c}_l} \bar{G}(\vec{s}, \vec{p}_l)\, d\vec{p}_l + \sum_i G(\vec{s}, \vec{p}_i) + B(\vec{s}) \quad (1)$$

where $G(\vec{s}, \vec{p})$ is the gradient at $\vec{s}$ due to a mass at $\vec{p}$ and $\bar{G}(\vec{s}, \vec{p}_l)$ is the gradient of the components of the gradient tensor. Removal of the background term

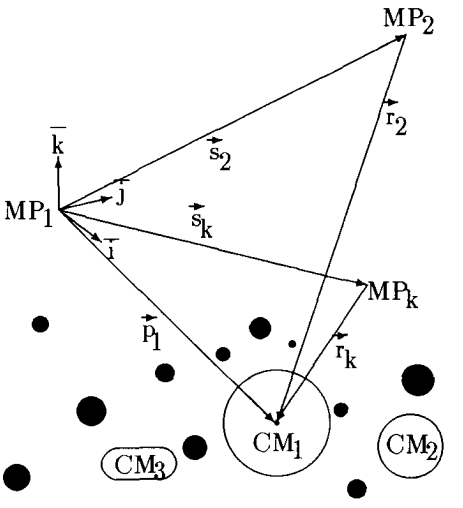

Figure 1: A model for a cut of the ground

$B(\vec{s})$ may be accomplished by assuming it is due to a spherical, uniformly dense mass M (the mass of the Earth) with center at a vertical distance R (the radius of the Earth). M and R may be either plugged in or estimated. Alternatively, we may only use measurements with the spinning wheel exactly in the xy-plane, since the readings do not depend on G_{zz}, G_{zy}, G_{zx}.

Equation (1) is not useful for our purposes unless one knows the exact number, location and nature of *all* the underground masses. Even if many of them can be disregarded because their effect is below "noise level", too much knowledge is still required to use (1). Moreover, there are several mass distributions that may produce the same gradient map. This non-uniqueness is inherent to the problem and can be circumvented through adequate modeling hypotheses.

We propose to model the gradient at a measurement point as if it were due to a few candidate patterns of mass, whose intensities and locations are to be determined. The unmodeled gradient is attributed to an extra term playing the role of noise. Then the model equation for the gradient at the MP, $\vec{s}$, is

$$G(\vec{s}) = \sum_{l \in \mathcal{L}} \int_{\vec{c}_l} \bar{G}(\vec{s}, \vec{p}_l)\, d\vec{p}_l + \sum_{i \in \mathcal{I}} G(\vec{s}, \vec{p}_i) + B(\vec{s}) + e \quad (2)$$

where $\mathcal{L}$ and $\mathcal{I}$ are the index sets for the chosen distributed and point masses, respectively. Some physical reasoning, see [4], indicates that a good assumption for e is that it is white Gaussian noise, of zero mean and variance σ^2. In our model the vertical component of $B(\vec{s})$ is large enough that the probability of having a negative vertical component of $G(\vec{s})$ is almost zero.

There are several mass patterns of interest. For instance, the simplest pattern resembling a tunnel is, perhaps, a linear mass density of a certain length. More concentrated objects with higher densities can be better modeled by a simple point mass. If the same mass is close to the surface, then concentrating it into a point mass may not be accurate enough and a distributed mass model may be needed. For those cases when the shape of the object becomes important, a multipole expansion is probably needed [2]. An account of this issue is presented in [4]. For brevity, we shall only derive the case of point masses.

Suppose there is a point source of mass m_1, located at $\vec{p}_1$ with respect to a reference frame $(\bar{i}, \bar{j}, \bar{k})$ and the sensor is placed at the point $\vec{s}_k$, see fig. 1. Using elementary physics for the gravitational field components in terms of the vector $\vec{r}_k \triangleq \vec{p}_1 - \vec{s}_k$, we can write

$$\begin{aligned} F_x(\vec{s}_k) &= \gamma m_1 \frac{\vec{r}_k \cdot \bar{i}}{\mid \vec{r}_k \mid^3} \\ F_y(\vec{s}_k) &= \gamma m_1 \frac{\vec{r}_k \cdot \bar{j}}{\mid \vec{r}_k \mid^3} \\ F_z(\vec{s}_k) &= \gamma m_1 \frac{\vec{r}_k \cdot \bar{k}}{\mid \vec{r}_k \mid^3} \end{aligned}$$

The gradient is obtained differentiating with respect to the components of $\vec{s}_k$:

$$\text{vech}\{G(\vec{s}_k)\} = \frac{\gamma m_1}{\mid \vec{r}_k \mid^5} \begin{bmatrix} 3(\vec{r}_k \cdot \bar{i})^2 - \mid \vec{r}_k \mid^2 \\ 3(\vec{r}_k \cdot \bar{i})(\vec{r}_k \cdot \bar{j}) \\ 3(\vec{r}_k \cdot \bar{i})(\vec{r}_k \cdot \bar{k}) \\ 3(\vec{r}_k \cdot \bar{j})^2 - \mid \vec{r}_k \mid^2 \\ 3(\vec{r}_k \cdot \bar{k})(\vec{r}_k \cdot \bar{j}) \\ 3(\vec{r}_k \cdot \bar{k})^2 - \mid \vec{r}_k \mid^2 \end{bmatrix} \qquad (3)$$

with $\text{vech}\{G(\vec{s}_k)\} \triangleq [G_{xx}\ G_{xy}\ G_{xz}\ G_{yy}\ G_{yz}\ G_{zz}]^T_{|\vec{s}_k}$. Note that the components G_{xx}, G_{yy} and G_{zz} sum to zero, reflecting Poisson's equation.

We define the response vector from the "source" m_1 to the gradient $g_j(k)$ as:

$$a_{jk}(\boldsymbol{\theta}_1) = \mathbf{M_j}\ \text{vech}\{G(\vec{s}_k)\}/m_1 \qquad (4)$$

with location parameter vector $\boldsymbol{\theta}_1 \triangleq (\vec{p}_1 \cdot \bar{i},\ \vec{p}_1 \cdot \bar{j},\ \vec{p}_1 \cdot \bar{k})$ and then we get the form $g_j(k) = a_{jk}(\boldsymbol{\theta}_1)m_1$. According to eqn. (2), the output of the gradiometer at instant t is $y_{jk}(t) = g_j(k) + e_{jk}(t)$.

It can be seen that m_1 is unidentifiable or not uniquely separable from $a_{jk}(\boldsymbol{\theta}_1)$, *i.e.* if we have a mass m_1 located at distance $\mid \vec{r}_k \mid$ from $\vec{s}_k$, then a mass of size qm_1 located at $q^{1/3}\vec{r}_k$ produces the same gradient tensor. However, measuring at a different point $\vec{s}_2$, such that $\vec{p}_1 - \vec{s}_1$ is not co-linear with $\vec{p}_1 - \vec{s}_2$, resolves the ambiguity. This is a simple interesting example of how having different measurement points may help thinning the non-uniqueness of the inverse problem.

3 Parameter Estimation Approach

We use a maximum likelihood procedure to estimate point-mass parameters and compute the CRB to assess the quality of our location estimates of spheroidal mass objects. If we take measurements at one MP only five parameters can be estimated, since there are five independent components of the gradient. Therefore, any practical situation must include several MP's to provide enough equations. Consider a situation where we select K measurement points and J sensor orientations. For simplicity, we assume the same number of sensor orientations and the same number, N, of time repetitions for each MP. We consider a model with d point masses. The equivalent to a "snapshot" in an array is given by

$$\begin{aligned} Y(t) &= \left[y^T_{11}(t),\ \cdots,\ y^T_{J1}(t),\ \cdots,\ y^T_{JK}(t)\right]^T = \\ &= \mathbf{A}(\boldsymbol{\theta})\mathbf{x} + \mathbf{e}(t) \end{aligned}$$

of dimension $m \times 1$, with $m = 2JK$, and $\mathbf{x} = [m_1\ \cdots\ m_d]^T$ and where the equivalent to the "array manifold" is

$$\mathbf{A}(\boldsymbol{\theta}) = [a(\boldsymbol{\theta}_1)\ a(\boldsymbol{\theta}_2)\ \cdots\ a(\boldsymbol{\theta}_d)] \qquad (5)$$

The parameters to be estimated are $(\boldsymbol{\theta}^T, \mathbf{x}^T, \sigma^2)$. Their total number is $n_p = 4d+1$, *i.e.* $n \triangleq 3d$ parameters from $\boldsymbol{\theta}$, d from $\mathbf{x}$ and 1 from σ.

When other patterns are included, we still can give the problem the structure of the previous equations. Unfortunately the number of parameters to be estimated grows rapidly, risking the performance, see [4]. Increasing the number of MP's is important not only because of noise reduction but also as a way of refining our model regarding the non-uniqueness of the inverse problem, as seen in the previous section.

Assume the noise term $\mathbf{e}(t)$ is Gaussian distributed with zero mean and covariance $\sigma^2\mathbf{I}_m$. Thus, $Y(t)$ is a discrete-time Gaussian stochastic process with mean $\mathbf{A}(\boldsymbol{\theta})\mathbf{x}$ and covariance $\sigma^2\mathbf{I}_m$. The log-likelihood function of the N-size sample is

$$-N\left(m\ln(2\pi) + \ln|\mathbf{R}(\boldsymbol{\theta})| + \text{trace}\left\{\mathbf{R}(\boldsymbol{\theta})^{-1}\hat{\mathbf{R}}(\boldsymbol{\theta})\right\}\right)$$

$$\begin{aligned} \mathbf{R}(\boldsymbol{\theta}) &= \mathrm{E}\left\{(Y(t) - \mu(\boldsymbol{\theta}))\,(Y(t) - \mu(\boldsymbol{\theta}))^T\right\} = \sigma^2\mathbf{I}_m \\ \hat{\mathbf{R}}(\boldsymbol{\theta}) &= \frac{1}{N}\sum_{t=1}^{N}(Y(t) - \mathbf{A}(\boldsymbol{\theta})\mathbf{x})\,(Y(t) - \mathbf{A}(\boldsymbol{\theta})\mathbf{x})^T \\ \mu(\boldsymbol{\theta}) &= \mathrm{E}\{Y(t)\} = \mathbf{A}(\boldsymbol{\theta})\mathbf{x} \end{aligned}$$

It can be shown that the following statistics:

$$\tilde{\mu} = \frac{1}{N}\sum_{t=1}^{N} Y(t)$$

$$\mathbf{s}_N^2 = \frac{1}{N}\sum_{t=1}^{N} Y^T(t)Y(t)$$

are sufficient for this problem. The maximum likelihood estimate of the parameters $(\boldsymbol{\theta}, \mathbf{x}, \sigma^2)$ can be easily found as in [6], or using concentrated likelihood function concepts, as in [1], obtaining

$$\begin{aligned}\hat{\boldsymbol{\theta}} &= \operatorname{argmin}\left\{\ln\left(\mathbf{s}_N^2 - \tilde{\mu}^T P_A(\boldsymbol{\theta})\tilde{\mu}\right)\right\} \\ \hat{\mathbf{x}} &= \left[\mathbf{A}^T(\hat{\boldsymbol{\theta}})\mathbf{A}(\hat{\boldsymbol{\theta}})\right]^{-1}\mathbf{A}^T(\hat{\boldsymbol{\theta}})\tilde{\mu} \\ \hat{\sigma}^2 &= \left(\mathbf{s}_N^2 - \tilde{\mu}^T P_A(\boldsymbol{\theta})\tilde{\mu}\right)/m\end{aligned}$$

where $P_A(\boldsymbol{\theta})$ is the projection matrix onto the column space of $\mathbf{A}(\hat{\boldsymbol{\theta}})$ (see [6]). The optimization problem for $\boldsymbol{\theta}$ requires a multidimensional non-linear minimization procedure and suffers from the standard difficulties, such as multiple minima, choice of initial condition and computational time. Observe that, unlike the deterministic case of the classical source localization problem (see [7]), our case has a constant source signal, resulting in slightly different estimation formulas.

The Cramér-Rao bound (CRB), assuming unbiased estimates, can be derived as in [7], or taking advantage of the concentrated structure of the likelihood function, as in [1]. We obtain the following bounds (see [7])

$$\begin{aligned}\mathrm{CRB}(\sigma^2) &= \frac{\sigma^4}{Nm} \\ \mathrm{CRB}(\mathbf{x}) &= \frac{\sigma^2}{4N}\left(\mathbf{A}^T(\boldsymbol{\theta})P^{\perp}_{(\mathbf{X}\mathbf{D}(\boldsymbol{\theta}))^T}\mathbf{A}(\boldsymbol{\theta})\right)^{-1} \\ \mathrm{CRB}(\boldsymbol{\theta}) &= \frac{\sigma^2}{4N}\left(\mathbf{X}\mathbf{D}(\boldsymbol{\theta})P^{\perp}_{\mathbf{A}(\boldsymbol{\theta})}\mathbf{D}^T(\boldsymbol{\theta})\mathbf{X}^T\right)^{-1}\end{aligned}$$

where we have defined

$$\begin{aligned}\mathbf{X} &= \mathbf{I}_n \otimes \mathbf{x}^T \qquad (n \times dn) \\ \mathbf{D}(\boldsymbol{\theta}) &= \left[\begin{array}{ccc} \frac{\partial \mathbf{A}(\boldsymbol{\theta})}{\partial \theta_1} & \cdots & \frac{\partial \mathbf{A}(\boldsymbol{\theta})}{\partial \theta_n} \end{array}\right]^T \quad (dn \times m)\end{aligned}$$

The latter matrix can be obtained, in our case of point masses, by differentiating the formulas of eqn (5) using (4) and (3). As is well known, our maximum likelihood estimator need not be unbiased nor achieve the CRB. However, we shall use the CRB to give us an indication of the best possible performance for unbiased estimates.

4 Simulations and Results

We have conducted several studies that illustrate, in figures 2 to 5, the range of possibilities of our procedure. In all cases it was assumed that the mass was

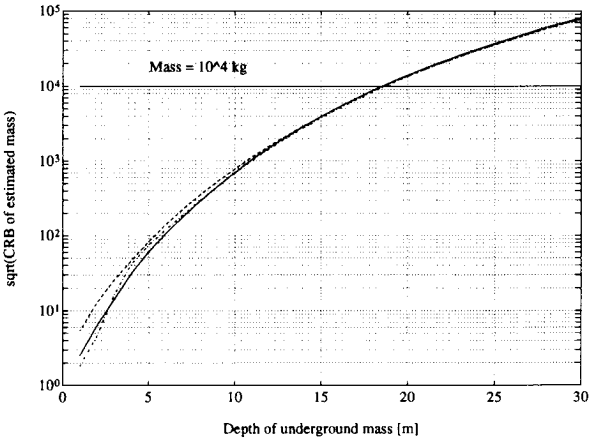

Figure 2: CRB of the estimated mass for a point mass at a variable depth

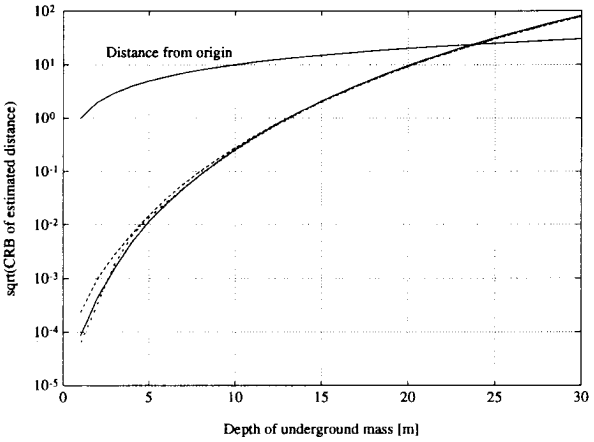

Figure 3: CRB of the estimated location of a point mass at variable depth

of 10^4Kg, a noise of $\sigma = 1\mathrm{E}$ (the level of the electronic noise) and $N = 100$ time samples were taken. Three orientations of the gradiometer were used, one along each co-ordinate axis. Four patterns of five MP's each, all on the surface $(z = 0)$, were chosen with (x, y) co-ordinates given by

	$\vec{s}_1$	$\vec{s}_2$	$\vec{s}_3$	$\vec{s}_4$	$\vec{s}_5$
—	$(-4,0)$	$(-2,0)$	$(0,0)$	$(2,0)$	$(4,0)$
···	$(0,-4)$	$(0,-2)$	$(0,0)$	$(0,2)$	$(0,4)$
– · –	$(-3,-3)$	$(-1,-1)$	$(0,0)$	$(1,1)$	$(3,3)$
– – –	$(-1,-3)$	$(1,-1)$	$(2,0)$	$(3,1)$	$(5,3)$

The first column indicates how they show up in the figures. In fig. 2 we show the CR standard deviation bound for an estimate of the mass as a function of the

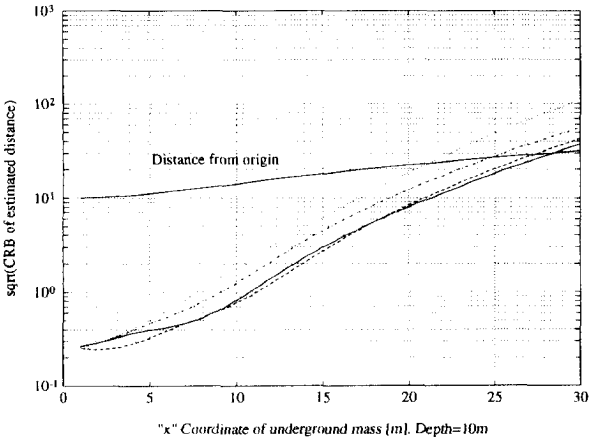

Figure 4: CRB of the estimated location of a point mass at a variable "x" and a depth of 10 meters

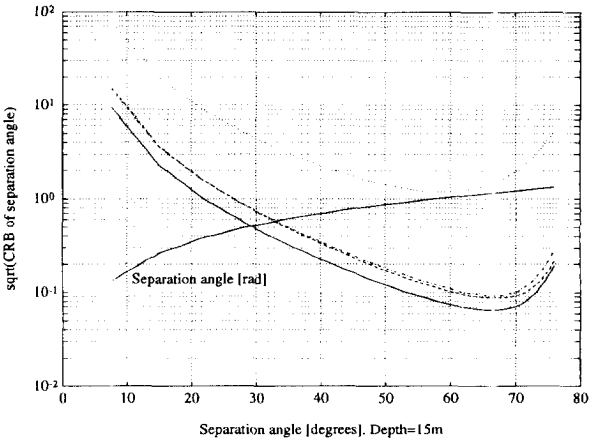

Figure 5: CRB of the estimated separation angle for two equal masses at a depth of 15 meters

depth at which the point mass is located. If we assume that the estimates are useful until their standard deviation is about a third of the value to be estimated, then the method can be used up to a depth of 15 meters. From fig. 3 we can see that a similar limit exists when estimating the range of the point mass. All the patterns of MP perform similarly. This situation changes when, as fig. 4 shows, the point mass is shifted in the x direction. Then, as it may be expected from physical principles, the arrays of MP with components along the x axis perform better. The example of fig. 5 is on the resolution of two point masses of 10^4Kg separated by a variable angle, at a depth of 15 meters. We see how the pattern of MP along the y axis fails to resolve them, whereas all other arrays of MP separate the masses for angles larger than 40 degrees. If the masses were not so deep, they could be resolved for smaller angles.

5 Summary and Conclusions

We have presented a procedure that allows the characterization of underground sources of mass, based on measurements of the gravitational gradient with a spinning wheel sensor. Applications may call for different modeling hypotheses, but for brevity we only showed the case of point masses. CRB derived limits show an ample potential for applications.

References

[1] B. Hochwald and A. Nehorai, "Concentrated Cramér-Rao Bound Expressions," *IEEE Trans. on Information Theory,* Vol. 40, pp. 363-371, March 1994.

[2] J.D. Jackson, "*Classical Electrodynamics*", 2nd. Edition, John Wiley, 1975.

[3] E.H. Metzger, "Development Experience of Gravity Gradiometer System", *IEEE Plans Meeting*, 1982.

[4] C.H. Muravchik and A. Nehorai, "Localization and Identification of Underground Objects using Gravitation Measurements", *to be submitted.*

[5] J. Parmentola, "The Gravity Gradiometer as a Verification Tool", *Science and Global Security*, vol. 2, pp. 43-57, 1990.

[6] B. Porat, *Digital Processing of Random Signals: Theory and Methods*, Prentice Hall, Englewood Cliffs, NJ, 1994.

[7] P. Stoica and A. Nehorai, "MUSIC, Maximum Likelihood and Cramer-Rao Bound", *IEEE Trans. Acoust. Speech, Signal Processing*, vol. 37, pp. 720-741, May 1989.